Progress In Electromagnetics Research C, Vol. 97, 241–253, 2019

The Design of a Compact Quintuple Band-Notched UWB Antenna

Xia Cao[1, 2], Yingqing Xia[1, *], Ling Wu[3], Lei Lang[1], and Li Cui[1]

Abstract—Due to suppressing the interference from WLAN (2.4–2.484 GHz), WiMAX (3.3–3.7 GHz), INST (4.5–4.8 GHz), X-band (7.25–7.75 GHz), and ITU band (8.01–8.5 GHz) signals in ultra-wideband (UWB) communication systems, a novel UWB antenna with five notch bands is proposed. Based on the methodologies of loading parasitic stubs and etching slots, the antenna is designed with five band rejection elements: a curved stub, a split square ring-shaped slot and a pair of vertical slots introduced in the patch, two C-shaped stubs symmetrically set near the feed line, and a pair of L-shaped slots etched on the ground plane. The test results show that the antenna operating from 1.95 to 10.73 GHz is capable of rejecting the frequency bands around 2.4 GHz, 3.5 GHz, 4.6 GHz, 7.5 GHz, and 8.4 GHz. Meanwhile, in passbands the antenna has approximate omnidirectional radiation patterns and a peak gain higher than 1.7 dBi. The proposed antenna with dimensions of $31 \times 35 \times 1.5\,\text{mm}^3$ is simple in structure and meets the requirements of UWB systems applications.

1. INTRODUCTION

In 2002, the UWB technology was approved by FCC for civilian use, and frequency band from 3.1 to 10.6 GHz was classified as a usable band for UWB communication systems. With such advantages as high speed, low power consumption, and little interference, UWB communication technology has experienced prompt development in the field of wireless communication. As a key component of a UWB communication system, UWB antenna has also become a hot research topic. In consideration of the existence of narrowband communication systems in the UWB bands, the UWB antenna with band-notched characteristics is a simple and effective solution to restrain these interference signals for UWB communication [1].

The simplest and most widely used method for obtaining band notch characteristics is to load different types of parasitic elements or etch slots on the UWB antenna [2]. In previous studies, some excellent band-notched antennas based on these methods have been introduced. For example, multiband suppression is obtained by opening suitable slots in radiation patches [3–9]. In [3], a 5.5 GHz WLAN notch band is introduced by etching four CSRR structures. Three rectangular slots [4], three U-shaped slots [5], and two L-shaped slots [6] are etched to produce dual notch bands. Triple notch bands are obtained by etching a fractal Koch slot [7] and three C-shaped slots [8]. Three inverted U-shaped slots and a single I-shaped slot are cut to achieve band-notched characteristics at four frequency bands [9]. The slots in the antenna that cause band-notches can also be located on the ground plane and feed line [10–15]. To be exact, the antenna with two SRR slots [10] or C-shaped slots [11] has single stopband. Two pairs of meander three reject-bands are produced by inserting three square slots into the feed line [13]. By symmetrically placing three pairs of C-shaped slots on ground plane and etching a U-shaped slot and a C-shaped slot in radiating patch, the antenna has five band-notches [14]. Moreover, a combination of loading parasitic elements and etching slots is used in [16–20] to achieve multiple band

Received 12 September 2019, Accepted 26 November 2019, Scheduled 17 December 2019

* Corresponding author: Yingqing Xia (yingqingxia_ccnu@126.com).

[1] Department of Electronics and Information Engineering, Central China Normal University, Wuhan 430079, China. [2] Wuhan Qingchuan University, Wuhan, Hubei 430204, China. [3] School of Physics and Electronic Information Engineering, Hubei Engineering University, Xiaogan 432000, China.

notched characteristics. For example, two parasitic stubs are loaded on the patch and a U-shaped slot opened in the feed line to suppress the interference in WiMAX band (3.17–3.8 GHz) and ITU band (8–9.1 GHz) [16]. In [17], by placing two asymmetrical structures on both sides of the feed line, adding a pair of circular arc strips symmetrically at the bottom of the radiation patch, and cutting a pair of inverted L-shaped slots on the ground plane, triple notch bands are achieved. In addition, several special methods are introduced [21–25]. In [21], two pairs of SRR elements are printed on the back side of a CPW-fed monopole antenna to produce dual band notched characteristics. Four different structures of CSRR rings and a pair of SRR rings are distributed on the antenna to obtain five reject-bands [22]. EBG structures [23, 24] and an electric ring resonator [25] are used to create stopband characteristics. It is a difficult task to introduce more notch elements in the limited space of a miniaturized UWB antenna and space the notch elements properly so as to reduce the mutual coupling between them, which will undoubtedly increase the difficulty of debugging. Therefore, there are almost no more than five notch bands in the literature about notch antenna design, and only a few of these studies have realized quintuple-notched characteristics.

In this paper, quintuple-notched characteristics are realized on a UWB antenna by adding a curved stub, opening a split square ring-shaped slot and a pair of vertical strip slots in the patch, as well as putting a pair of C-shaped stubs at each side of the feed line and symmetrically opening two L-shaped slots in the ground plane. On this basis, the dimensions of each structure are adjusted to effectively reject signals of IEEE 802.11b/g/n WLAN (2.4–2.484) GHz, WiMAX (3.3–3.7 GHz), INST (4.5–4.8 GHz), Satellite Communication System downlink X-band (7.25–7.75 GHz), and ITU (8.01–8.5 GHz). Compared with the previous work, the antenna has a smaller size than the quintuple band-notched antenna ($38 \times 36\,\text{mm}^2$) reported in [14] and uses much cheaper substrate materials than the penta-notched antenna in [22] which uses Rogers materials. The designed antenna is compact, and it uses a simpler notch structure which allows for better isolation and more convenient debugging than [14, 22]. The major parameters and properties of the representative antenna mentioned above are collected in Table 1.

2. ANTENNA DESIGN AND ANALYSIS

The antenna is printed on an FR-4 substrate, with relative dielectric constant ε_r 4.4, and the tangent of loss angle δ is 0.025. Two right triangles are excised on the edge of patch to expand the operating frequency band to 1.95–10.73 GHz. The width wf of 50 Ω microstrip line is calculated by simulation software CST, which is set to 2.8 mm. There are five notch structures (ST1–ST5) in the antenna to achieve quintuple band-notched characteristics at bands of 2.08–2.87 GHz, 3.2–3.82 GHz, 4.35–4.83 GHz, 6.98–7.73 GHz, and 7.91–8.66 GHz. It is necessary to rationally arrange the position of each structure and adjust the corresponding dimensions. The configurations of this designed antenna and five notch structures are shown in Fig. 1, and final dimensions optimized by simulation software CST are listed in Table 2. The operating mechanism and parameter analysis of the proposed antenna are presented in the following parts.

2.1. Design Principle and Procedure

The impedance and radiation characteristics of basic UWB antenna will change with the addition of resonant structure. When the total length Ls of the structure approximates a quarter or half of the center frequency wavelength λ_g in suppressed band, the antenna produces a larger reflection in this band. Thus the desired notch characteristics can be achieved. The wavelength λ_g is determined by Eq. (1), where C denotes the light velocity, and ε_r represents the relative dielectric constant of the substrate.

$$\lambda_g = \frac{C}{f_r\sqrt{\dfrac{\varepsilon_r + 1}{2}}} \tag{1}$$

The proposed antenna obtains five notch bands by introducing ST1–ST5, and the length of these five structures are taken as $Ls1 = L1+L2+L3+W1+W2+W3$, $Ls2 = L5+W5$, $Ls3 = 2*(L4+W4)-G1$, $Ls4 = 2*W6+L6$, and $Ls5 = L7$. Among them, ST1, ST3, and ST4 are one-half wavelength

Table 1. Comparison of the proposed antenna with other existing antennas.

Refs.	Size (mm^2)	Notched bands (GHz)	Substrate	Band Width (GHz)	Main method
[4]	26×30	5.15–5.82 7.25–8.39	FR-4	3.15–10.63	Etching slots
[7]	50×50	1.95–2.25 3.15–3.65 5.4–6.0	FR-4	1.78–11	Etching slots
[10]	78×44.6	5.12–6.77	FR-4	2.44–10.79	Etching slots
[12]	78×80	2.15–2.65 3.0–3.7 5.45–5.95 8.0–8.68	FR-4	1.5–12	Etching slots
[14]	36×38	3.45–4.0 5.15–5.9 6.77–8.0 8.3–9.1 9.3–10.6	FR-4	2.86–13.3	Etching slots
[16]	23×32	3.17–3.85 8.0–9.1	FR-4	2.57–11.3	Loading stubs and Etching slots
[17]	30×30	3.39–3.88 5.11–5.97 8.0–8.71	FR-4	3.0–12	Loading stubs and Etching slots
[22]	30×28	3.3–3.5 5.15–5.35 5.725–5.8 6.85–7.4 7.6–8.1	RO4003	3–10	Metamaterial structure
[23]	38×40	3.36–3.85 5.2–5.9	FR-4	2.8–12	EBG
This work	31×35	2.08–2.87 3.2–3.82 4.35–4.83 6.98–7.73 7.91–8.66	FR-4	1.95–10.73	Loading stubs and Etching slots

resonant structures at 2.4 GHz, 4.5 GHz, and 7.5 GHz, respectively; the rest ST2 and ST5 are one-quarter wavelength resonant structures at 3.5 GHz and 8.4 GHz, respectively. Fig. 2 and Fig. 3 show the evolution of the quintuple band-notched antenna and the corresponding reflection coefficient at each stage. It is observed that each additional structure introduces a corresponding notch band. According to the above principles, the theoretical calculated length and optimized length of these five elements are listed in Table 3. The comparison between them shows a small difference, which means that the design method is feasible. In the next, the effect of the adjustment of the resonator length on the notch band is discussed.

Table 2. Final dimensions of the designed antenna.

Para.	Size (mm)	Para.	Size (mm)	Para.	Size (mm)	Para.	Size (mm)
W_s	31	W_{p1}	9.2	L_2	3.1	W_5	3.2
L_s	35	W_{p2}	0.4	L_3	2	L_5	9.8
W_f	2.8	W_{p3}	2.5	S_1	0.5	S_3	0.6
L_f	14	W_1	10.3	W_4	6.7	W_6	4.3
W_r	13.8	W_2	8.3	L_4	5.6	L_6	4.3
L_r	15	W_3	6.3	S_2	0.3	S_4	0.4
L_g	13	L_1	4	G_1	1.5	L_7	5.4
S_5	0.3						

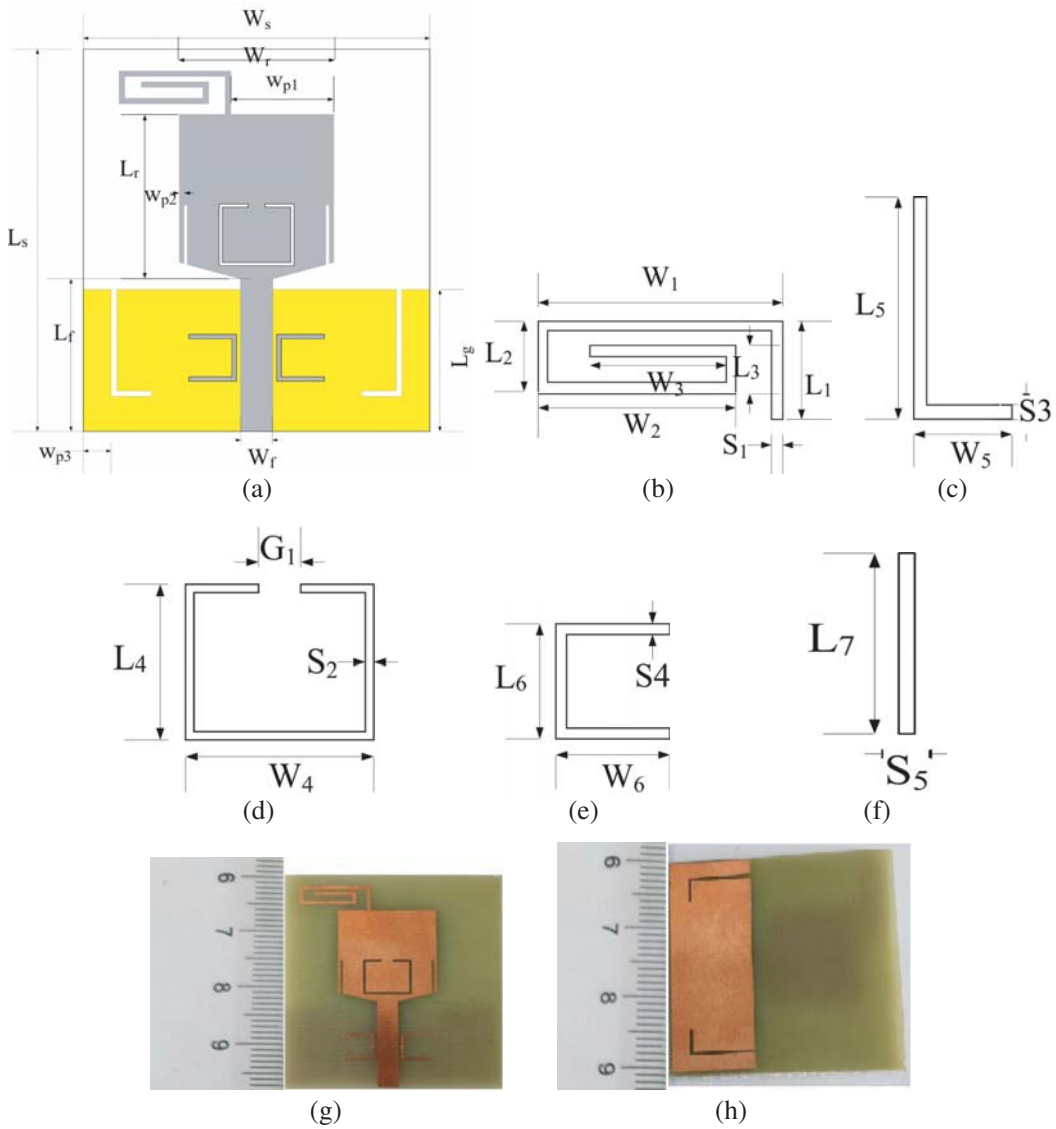

Figure 1. Configuration of the designed antenna. (a) Overall model. (b) Stub ST1. (c) Slot ST2. (d) Slot ST3. (e) Stub ST4. (f) Slot ST5. (g) Front of fabricated antenna. (h) Back of fabricated antenna.

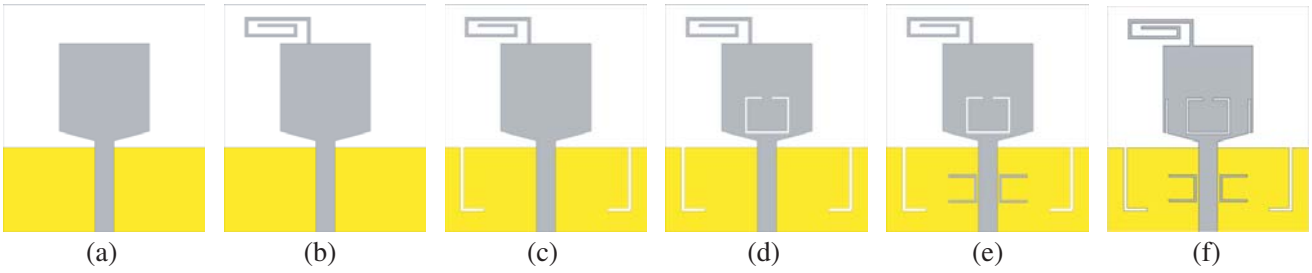

Figure 2. The evolution of the design. (a) Ant-1. (b) Ant-2. (c) Ant-3. (d) Ant-4. (e) Ant-5. (f) Proposed Ant.

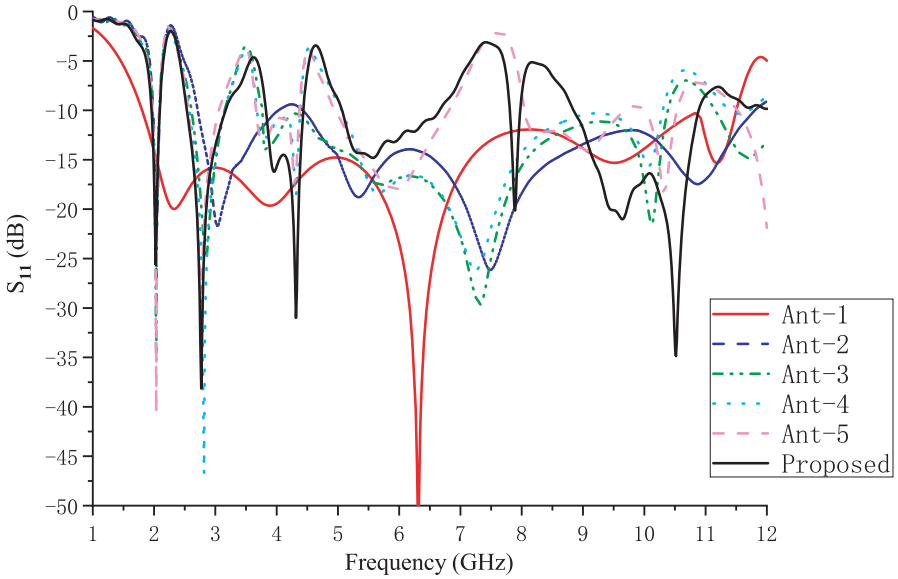

Figure 3. Simulated S_{11} of the antenna at six stages.

Table 3. Comparison of length between calculation and simulation.

Length	Notched frequency (GHz)	Calculation size (mm)	Simulation size (mm)
L_{s1}	2.4	38	37
L_{s2}	3.5	13	13
l_{s3}	4.6	19.9	21.7
L_{s4}	7.5	12.2	12.9
l_{s5}	8.4	5.4	5.4

2.2. Parametric Study

The key parameters such as $W1$, $L5$, $G1$, $W6$, and $L7$ in each unit are studied. During parameter adjustment, one parameter is controlled, while the others are fixed. As can be seen from Figs. 4(a)–(e), when these parameter changes cause the structure length to increase, the corresponding notch band shifts toward lower frequency. Take $W1$ of ST1 as an example, as shown in Fig. 4(a), with the $W1$ increasing from 10 mm to 10.6 mm, the reflection coefficient S_{11} shifts toward the left side of 2.4 GHZ, and there is little influence on other notch bands. It should be noted that for two relatively close notch bands, the length adjustment range is limited. As shown in Fig. 4(d), when W6 of the ST4 is reduced

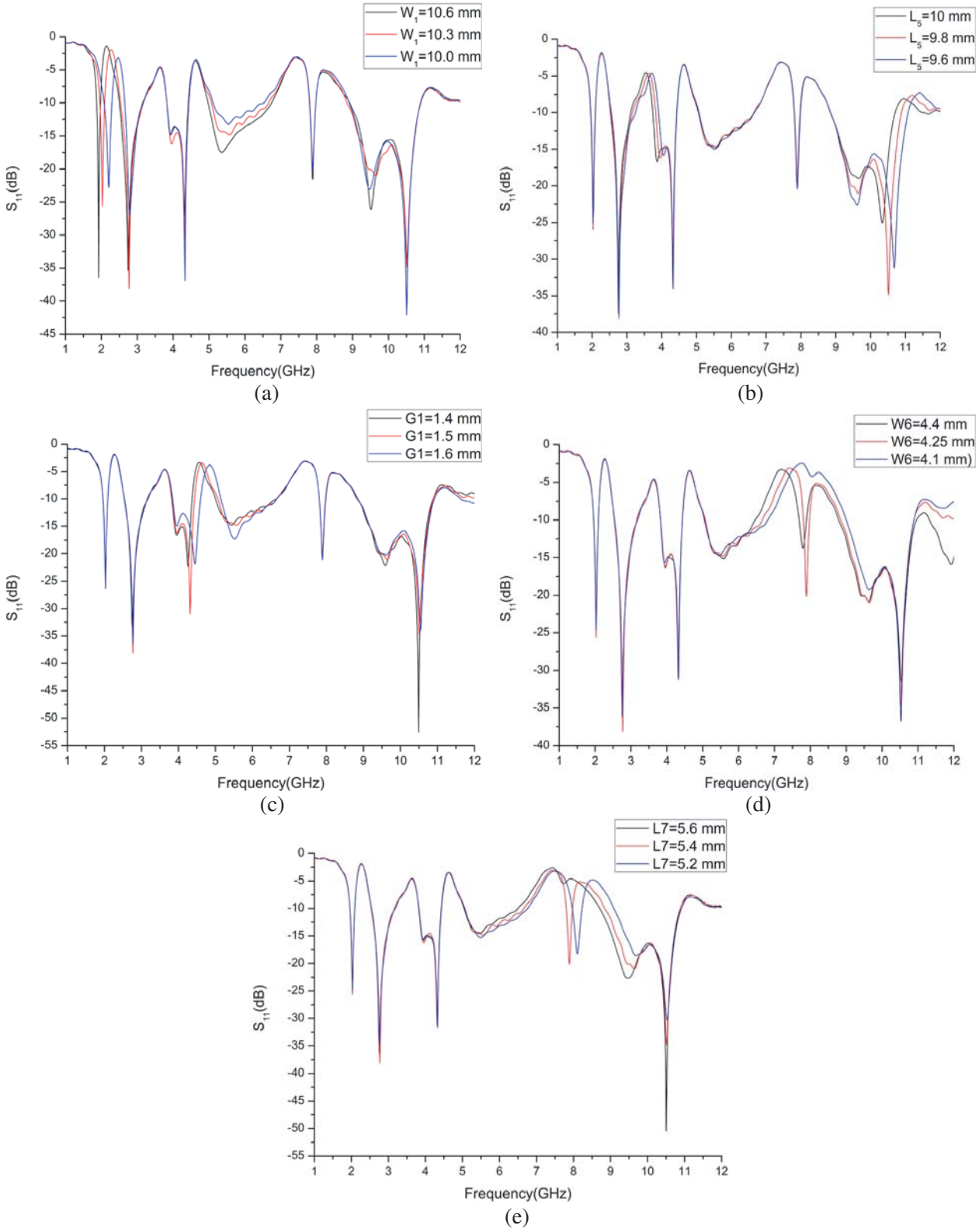

Figure 4. Simulated reflection coefficients for various value of the key dimensions. (a) The change of the $W1$. (b) The change of the $L5$. (c) The change of the $G1$. (d) The change of the $W6$. (e) The change of the $L7$.

from 4.4 to 4.1 mm, and the notch band around 7.5 GHz shifts to high frequency and interferes with the 8.4 GHz IUT band.

2.3. Surface Current Distribution and Equivalent Circuit Analysis of the Antenna

To further verify and analyze band-notched properties, the current distribution and input impedance curve of the antenna are simulated. As depicted in Fig. 5, current distribution is uniform at the operating frequency of 3 GHz, so the antenna works normally. However, the surface current concentrates on the corresponding notch structure at five notch frequencies, which leads to antenna impedance mismatch.

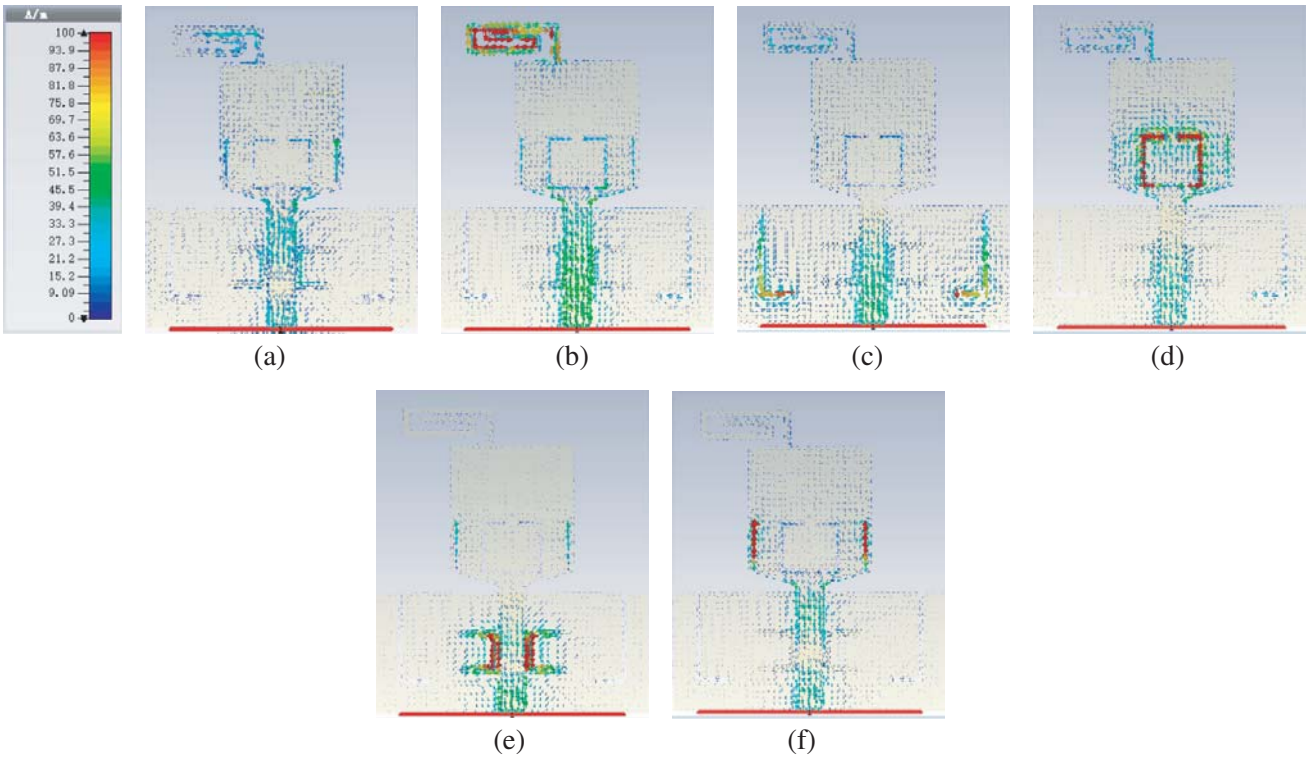

Figure 5. Surface current distributions at four resonant frequencies. (a) 3.0 GHz. (b) 2.4 GHz. (c) 3.5 GHz. (d) 4.6 GHz. (e) 7.5 GHz. (f) 8.4 GHz.

At the same time, the impedance characteristics are studied. As shown in Fig. 6, the impedances near 2.4 GHz, 3.5 GHz, and 7.5 GHz are similar to the series resonant circuit, because their reactances tend to zero, and reactance derivatives are positive. In addition, the resistance is a local valley. When the antenna works at 4.6 GHz and 8.4 GHz, the resistance is very high, and the reactance tends to zero and has negative derivative. So parallel resonance is considered to have occurred in the antenna. Whether the antenna resonates in series or parallel mode at certain frequency, it will cause impedance mismatch, and the antenna energy cannot be transmitted or received normally. According to the above analysis, the RLC equivalent circuit of the antenna can be made [26]. As shown in Fig. 7, a curved stub ST1, a pair of L-shaped slots ST2, and a pair of C-shaped stubs ST4 are equivalent to three series resonant circuits, and the two parallel resonant circuits represent the split square ring-shaped slot ST3 and vertical slots ST5. R1–R5, L1–L5, and C1–C5 in the equivalent circuit are created by ST1–ST5 individually.

Lumped element parameters (R1–R5, C1–C5, and L1–L5) of equivalent model are determined in two steps. First, they are estimated according to the resonance frequency f_n and bandwidth BW of RLC circuit given by Eq. (2)–Eq. (4), and then equivalent circuit and impedance file of UWB antenna (Ant-1) are loaded in ADS software. The final circuit parameters listed in Table 4 are obtained through

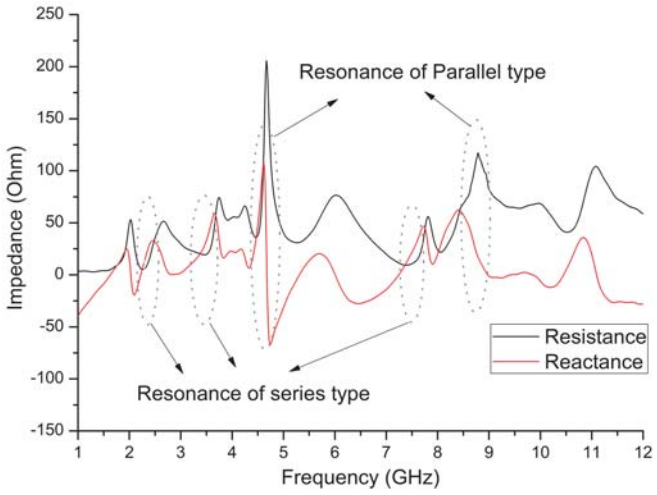

Figure 6. Input impedance of the antenna.

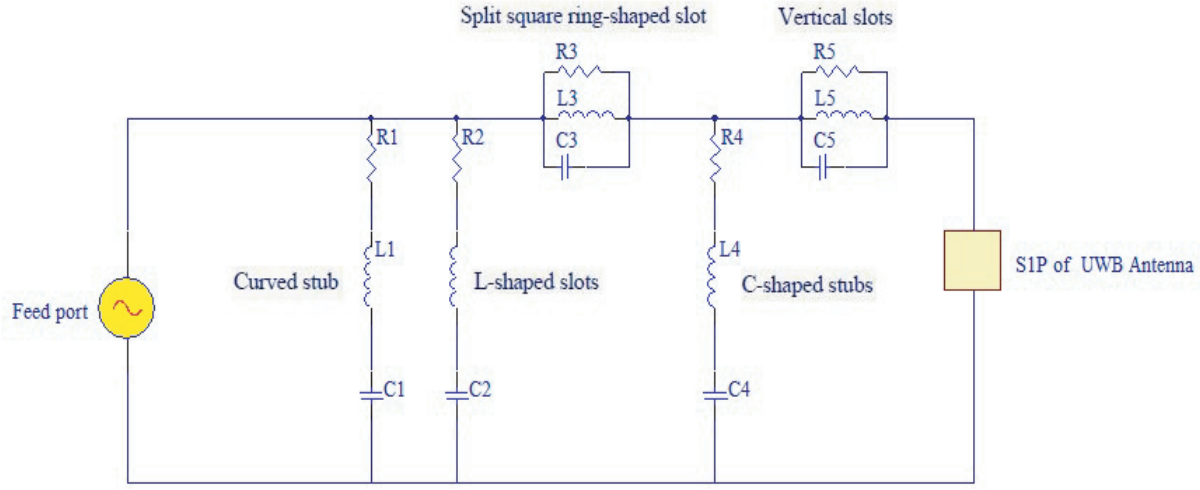

Figure 7. RLC equivalent circuit of the antenna.

Table 4. Component parameter values of the circuit model.

Circuit number	$f_{resonance}$ (GHz)	BW (GHz)	R (Ω)	C (ff)	L (nH)
1	2.4	0.79	18.9	97.72	43
2	3.5	0.62	21.6	61.16	34
3	4.6	0.48	226	22001	0.053
4	7.5	0.75	20.5	14.6	30.4
5	8.4	0.75	183	15126	0.024

optimization simulation. Comparing the reflection coefficient of the circuit with that of the proposed antenna, it can be seen from Fig. 8 and Fig. 12 that the notch frequencies of the two are identical, but the frequency bandwidth is slightly different. The results further illustrate the correctness of the design principle.

$$f_n = \frac{1}{2\pi\sqrt{L_n C_n}} \tag{2}$$

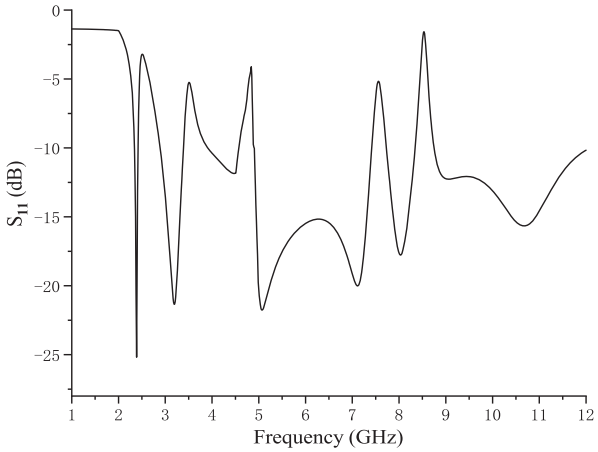

Figure 8. Reflection coefficient S_{11} of the equivalent circuit.

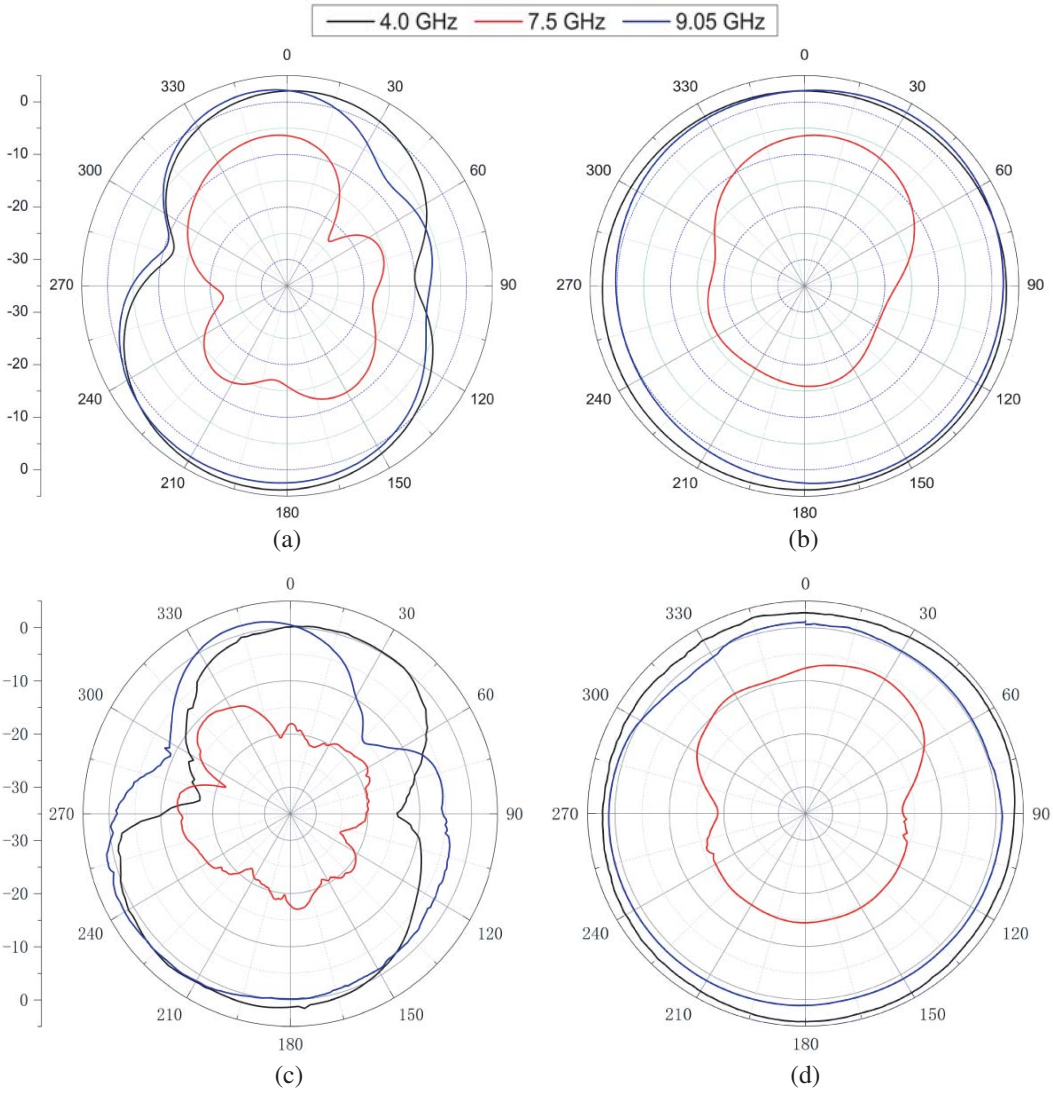

Figure 9. Radiation patterns of the proposed antenna. (a) E-plane (simulation). (b) H-plane (simulation). (c) E-plane (measurement). (d) H-plane (measurement).

$$BW_s = \frac{R_{ns}}{L_{ns}} \tag{3}$$

$$BW_p = \frac{1}{R_{np}C_{np}} \tag{4}$$

where BW_s and BW_p represent the bandwidth of series resonant circuit and parallel resonant circuit, respectively.

3. THE SIMULATED AND MEASURED RESULTS

The radiation characteristics and capabilities of the antenna are mainly described by the antenna radiation pattern, gain, and efficiency, which are obtained through simulation. As shown in Fig. 6, the radiation patterns of E-plane are approximate to 8-shape at the non-notch frequencies of 4 GHz and 9 GHz, which are similar to the traditional dipole antenna. Moreover, they are omnidirectional at H-plane generally. In contrast, the pattern is irregular at the rejection frequency of 7.5 GHz, and its gain is suppressed to about -10 dBi. Both the gain and efficiency are plotted in Fig. 10. The gain is above 1.7 dBi, and the efficiency is greater than 64% in passband, which illustrate that the antenna can receive and send signals effectively, whereas in the notch band, both the gain and efficiency decrease significantly, which are evidence of weakened radiation capability.

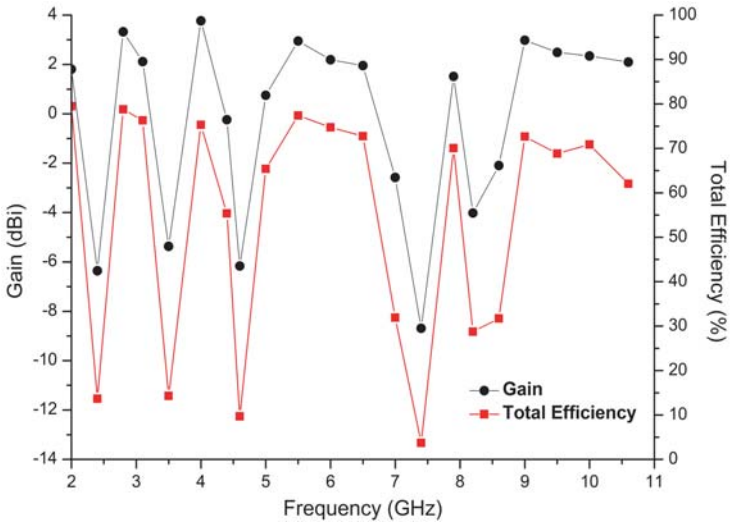

Figure 10. Simulated peak gain and efficiency of the proposed antenna.

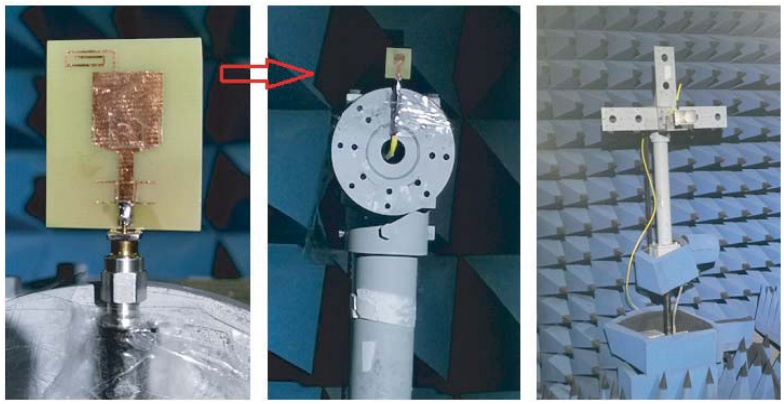

Figure 11. Measurement setup of the design.

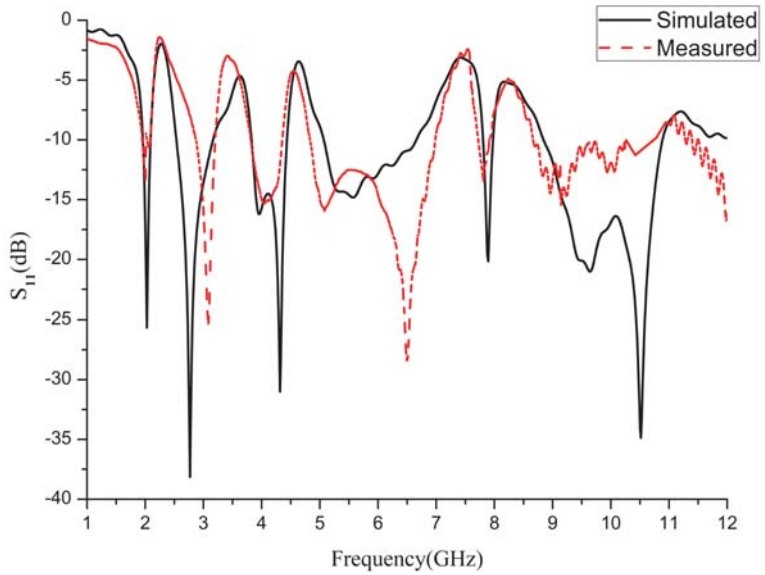

Figure 12. Simulated and measured reflection coefficients S_{11}.

For testing actual performance of the designed antenna, the antenna is fabricated according to the dimensions optimized through simulation (as shown in Fig. 1), and it is measured with the network vector analyzer Agilent E8362B. Fig. 8 shows the comparison of the S_{11} curves for antenna measurement and simulation, in which we can see that the measured and simulated reflectance coefficients are generally in line with each other. The deviations are due to the test environment, coaxial joint welding technology, and antenna processing errors, especially in the high frequency band, which is sensitive to dimension changes. Furthermore, in an anechoic chamber the radiation patterns measurement is carried out by using the horn antenna AVTADR2018 as a reference antenna. Photographs of measurement setup can been seen from Fig. 11. There is a high consistency between the simulated and measured radiation patterns as shown in Fig. 9.

4. CONCLUSIONS

In this paper, firstly a curved stub, a pair of L-shaped slots, a split square ring-shaped slot, a pair of C-shaped stubs, and a pair of vertical slots contributing to quintuple band-notched feature in the basic rectangular patch UWB antenna are designed and analyzed in terms of dimension study, surface current distribution, and equivalent circuit. After that, the proposed antenna is measured and simulated, and the results show that except for five notch bands (2.1–2.8 GHz, 3.2–3.8 GHz, 4.4–5 GHz, 6.7–7.8 GHz, 8–8.8 GHz), the reflectance coefficient S_{11} of the antenna is less than -10 dB within the 2–10.7 GHz band, and radiation characteristics are good. The antenna has a simple structure for debugging and repeating, moderate size, and satisfactory notch characteristics, which can meet the requirements of miniaturization and suppressing expected narrowband in UWB system. So, it has high practical value.

REFERENCES

1. Mouhouche, F., A. Azrar, M. Dehmas, et al., "Design a compact UWB monopole antenna with triple band-notched characteristics using EBG structures," *Frequenz*, Vol. 72, No. 11–12, 479–487, 2018.
2. Cao, P., J. Zhang, R. Alrawashdeh, et al., "Compact planar ultra-wideband antenna with quintuple band-notched characteristics," *IET Microwaves, Antennas & Propagation*, Vol. 9, No. 3, 206–216, 2015.

3. Mishra, G. and S. Sahu, "Compact circular patch UWB antenna with WLAN band notch characteristics," *Microwave and Optical Technology Letters*, Vol. 58, No. 5, 1068–1073, 2016.
4. Yadav, A., D. Sethi, and R. K. Khanna, "Slot loaded UWB antenna: Dual band notched characteristics," *AEU — International Journal of Electronics and Communications*, Vol. 70, 331–335, 2016.
5. Hu, Z., Y. Hu, Y. Luo, and W. Xin, "A novel rectangle tree fractal UWB antenna with dual band notch characteristics," *Progress In Electromagnetics Research C*, Vol. 68, 21–30, 2016.
6. Chandel, R., A. K. Gautam, and K. Rambabu, "Tapered fed compact UWB MIMO-diversity antenna with dual band-notched characteristics," *IEEE Transactions on Antennas and Propagation*, Vol. 66, No. 4, 21–30, 2018.
7. Zarrabi, F. B., Z. Mansouri, N. P. Gandji, et al., "Triple-notch UWB monopole antenna with fractal Koch and T-shaped stub," *AEU — International Journal of Electronics and Communications*, Vol. 70, No. 1, 64–69, 2016.
8. Sharma, M., Y. K. Awasthi, and H. Singh, "Design of compact planar triple band-notch monopole antenna for ultra-wideband applications," *Wireless Personal Communications*, Vol. 97, 3531–3545, 2017.
9. Mewara, H. S., D. Jhanwar, M. M. Sharma, et al., "A printed monopole ellipzoidal UWB antenna with four band rejection characteristics," *AEU — International Journal of Electronics and Communications*, Vol. 83, 222–232, 2018.
10. Tsai, L.-C. and W.-J. Chen, "A UWB antenna with band-notched filters using slot-type split ring resonators," *Microwave & Optical Technology Letters*, Vol. 58, No. 11, 2596–2598, 2016.
11. Ray, L. and M. R. Haider, "A compact planar self-affine sierpinski carpet fractal monopole antenna with band notch characteristics for ultra wideband communications," *Analog Integrated Circuits and Signal Processing*, Vol. 86, No. 3, 393–405, 2016.
12. Rehman, S. U. and M. A. S. Alkanhal, "Design and system characterization of ultra-wideband antennas with multiple band-rejection," *IEEE Access*, Vol. 5, 17988–17996, 2017.
13. Cai, Y. Z., H. C. Yang, and L. Y. Cai, "Wideband monopole antenna with three band-notched characteristics," *IEEE Antennas and Wireless Propagation Letters*, Vol. 13, 607–610, 2014.
14. Shankar Mewara, H., J. Kumar Deegwal, and M. Mohan Sharma, "A slot resonators based quintuple band-notched Y-shaped planar monopole ultra-wideband antenna," *AEU — International Journal of Electronics and Communications*, Vol. 83, 470–478, 2018.
15. Nazeri, A. H., A. Falahati, and R. M. Edwards, "A novel compact fractal UWB antenna with triple reconfigurable notch reject bands applications," *AEU — International Journal of Electronics and Communications*, Vol. 101, 1–8, 2019.
16. Guichi, F., M. Challal, and T. A. Denidni, "A novel dual band-notch ultrawideband monopole antenna using parasitic stubs and slot," *Microwave and Optical Technology Letters*, Vol. 60, No. 7, 1737–1744, 2018.
17. Wang, Z., J. Liu, and Y. Yin, "Triple band-notched UWB antenna using novel asymmetrical resonators," *AEU — International Journal of Electronics and Communications*, Vol. 70, 1630–1636, 2016.
18. Ali, W. A. E. and R. M. A. Moniem, "Frequency reconfigurable triple band-notched ultra-wideband antenna with compact size," *Progress In Electromagnetics Research C*, Vol. 73, 37–46, 2017.
19. Jin, Y., J. Tak, and J. Choi, "Quadruple band-notched trapezoid UWB antenna with reduced gains in notch bands," *Journal of Electromagnetic Engineering & Science*, Vol. 16, No. 1, 35–43, 2016.
20. Yadav, D., M. P. Abegaonkar, S. K. Koul, et al., "A compact dual band-notched UWB circular monopole antenna with parasitic resonators," *AEU — International Journal of Electronics and Communications*, Vol. 84, 313–320, 2018.
21. Siddiqui, J. Y., C. Saha, and Y. M. M. Antar, "Compact dual-SRR-loaded UWB monopole antenna with dual frequency and wideband notch characteristics," *IEEE Antennas and Wireless Propagation Letters*, Vol. 14, 100–103, 2015.

22. Muhibur, R., K. W. Tanveer, and I. Muhammad, "Penta-notched UWB antenna with sharp frequency edge selectivity using combination of SRR, CSRR, and DGS," *AEU — International Journal of Electronics and Communications*, Vol. 93, 116–122, 2018.
23. Mouhouche, F., A. Azrar, M. Dehmas, et al., "Design a compact UWB monopole antenna with triple band-notched characteristics using EBG structures," *Frequenz*, Vol. 72, No. 11–12, 479–487, 2018.
24. Jaglan, N., S. Dev Gupta, E. Thakur, et al., "Triple band notched mushroom and uniplanar EBG structures based UWB MIMO/diversity antenna with enhanced wide band Isolation," *AEU — International Journal of Electronics and Communications*, Vol. 90, 36–44, 2018.
25. Vendik, I. B., A. Rusakov, K. Kanjanasit, et al., "Ultra-Wideband (UWB) planar antenna with single-, dual-, and triple-band notched characteristic based on electric ring resonator," *IEEE Antennas and Wireless Propagation Letters*, Vol. 16, 1597–1600, 2017.
26. Wang, S. B. T., A. M. Niknejad, and R. W. Brodersen, "Circuit modeling methodology for UWB omnidirectional small antennas," *IEEE Journal on Selected Areas in Communications*, Vol. 24, No. 4, 871–877, 2006.